Journal of Applied Polymer Science

Inhibitory Effect of Hydrogen Bonding on Thermal Decomposition of the Nanocrystalline Cellulose/Poly(propylene carbonate) Nanocomposite

Jia-Li Hong, Xing-Hong Zhang, Ren-Jian Wei, Qi Wang, Zhi-Qiang Fan, Guo-Rong Qi
MOE Key Laboratory of Macromolecular Synthesis and Functionalization, Department of Polymer Science and Engineering, Zhejiang University, Hangzhou, 310027, China
Correspondence to: X. H. Zhang (E-mail: xhzhang@zju.edu.cn)

ABSTRACT: Biodegradable poly(propylene carbonate, PPC) is a typical noncrystalline polymer from the copolymerization of carbon dioxide (CO_2) with propylene oxide (PO). But it is easy to be degraded to propylene carbonate (PC) via backbiting route during heat process (above 170°C), which limits its application. This work reports the introduction of biodegradable nanocrystalline cellulose (NCC) which was exfoliated from microcrystalline cellulose (MCC) by acid hydrolysis into PPC, affording a biodegradable PPC/NCC nanocomposite with improved thermal decomposition temperatures (the initial decomposition temperature, $T_{5wt\%}$ was up to 265°C). Impressively, the thermal decomposition of PPC to PC at 200°C within 4.0 h was dramatically inhibited by introducing NCC, which was evident by ^{1}H NMR spectra. This could be attributed to the hydrogen bonding interaction between NCC and PPC. Moreover, the film of PPC/NCC nanocomposite had not deformed when it was heated at 110°C for 4 h. In application, such biodegradable nanocomposite is a promising disposable package material. © 2013 Wiley Periodicals, Inc. J. Appl. Polym. Sci. **2014**, *131*, 39847.

KEYWORDS: blends; cellulose and other wood products; degradation; polycarbonates

Received 3 June 2013; accepted 11 August 2013
DOI: 10.1002/app.39847

INTRODUCTION

Poly(propylene carbonate)(PPC) is synthesized by the alternating copolymerization of propylene oxide (PO) with carbon dioxide (CO_2),[1–4] as seen in Scheme 1. It is a very promising biodegradable polymer, because its synthesis meets with the principle of atom economy and its unique properties such as high transparency, biocompatibility, oxygen barrier properties and dielectronic properties.[5–7] Therefore, PPC is potential to be applied as the package materials, adhesives, solid electrolytes, photoresists and barrier materials etc.[8] Unfortunately, with the aliphatic carbonate linkages in this copolymer, PPC is easy to be degraded to propylene carbonate (PC) via backbiting mechanism[9] (see Scheme 2) at elevated temperatures especially more than 170°C.[1] This thermal degradation during processing significantly limits its application. As a result, the premise of PPC application is to develop method to overcome this problem.

By introducing the third monomers,[10–19] including lactide (LA),[10–12] cyclohexene oxide (CHO),[13–15] caprolactone (CL)[16–18] and γ-butyrolactone (BL)[19] into the PO-CO_2 copolymerization system, the thermal properties of the resultant terpolymers could be clearly improved. However, this method is considered to be high cost because introduction of the third monomer into the PO-CO_2 copolymerization system requires effective catalyst systems for keeping high monomers' conversion[11,14,20] and complex post-treatment method for purifying the product. To date, no effective catalysts were discovered for such terpolymerization, and no pilot production of such terpolymers was reported. Another effective chemical modification of PPC is capping the hydroxyl group of PPC by using anhydride or poly(styrene oxide-*co*-maleic anhydride) for inhibiting the backbiting degradation of PPC, since the end hydroxyl group caused the "unzipping" decomposition mode of PPC, as reported by Wang group.[21,22]

Blending of PPC with some synthetic polymers was effective for improving the thermal properties of PPC. Ethylene-vinyl alcohol(EVOH),[23] poly(lactic acid) (PLA)[24] and poly(vinyl alcohol) (PVA)[25] have been widely studied. Blending PPC with some non-biodegradable polymers will weaken the biodegradability of the resultant composites. Moreover, some degradable polymers such as PLA, when blended with PPC, needs to avoid the macrophase separation, which may deteriorate the mechanical properties. Generally, additives are required for improving the miscibility of both components. It is noted that the decomposition manner of PPC in a composite has been rarely reported. Natural polymers such as Starch[26–28] and wood flour[29] have

Scheme 1. The structure of poly (propylene carbonate) (PPC) from CO_2-PO copolymerization.

also been utilized to blend with PPC. However, the mechanical properties of these composites were less than that of pure PPC due to unsatisfied miscibility of both components.

Cellulose, as an important natural source material, widely exists in plant cell walls and some sea animals. It is a polysaccharide composed of $\beta-1$, 4—glucose units,[30,31] in which each repeat unit contains three hydroxyl groups, in which many hydrogen bonds with others is formed and make them stack on top of each other.[32] Microcrystalline cellulose (MCC) can be blended with PPC directly,[33] however, the noncrystalline part of MCC caused low thermal and mechanical properties of the resultant blends. Nanocrystalline cellulose (NCC), which has high crystallinity and present long rod-like material in a nanometer scale, can be obtained from acid/enzymatic hydrolysis of MCC of tunicin,[34–36] bacteria,[37] cotton,[38,39] wood,[40] and Avicel.[41] The width and length of NCC are generally 5–70 nm and 100nm–several micrometers, respectively. Because of its high crystallinity,[42] high Young's modulus,[30] high strength,[43] high surface area,[44] low coefficient of thermal expansion,[30] and biodegradability,[32] NCC is widely used as a reinforcement in polymer matrix such as PVC,[45] PVA,[33,46] and POE[47] to afford nanocomposites with improved properties.

Because noncrystalline PPC contains considerable amounts of carbonate units that are hydrogen-bond acceptor, and taking its biodegradability into accounts, NCC, which has highly crystallinity and present long rod-like material in a nanometer scale and many hydroxyl groups on its surface, is believed to be the ideal filler for modifying PPC, as shown in Figure 1. That is, introducing crystalline NCC into noncrystalline PPC, to construct a biodegradable PPC/NCC nanocomposite. Moreover, we hypothesized that the "unzipping" mode of PPC would be inhibited because the hydrogen bonding interaction of NCC and PPC, which is different to the "capping" method using anhydride or poly(styrene oxide-*co*-maleic anhydride) for improving the thermal properties of PPC. For testing the above hypothesis, in this work, we report the preparation of the PPC/NCC nanocomposites, and its decomposition behavior at high temperatures.

EXPERIMENTAL

Materials

PPC was prepared in our laboratory with carbonate content of 94%. The number-average molecule weight (M_n) and polydispersity index of PPC was 35,000 and 2.1(GPC, THF as a solvent, 35°C), respectively. Microcrystalline cellulose (MCC, cotton) was purchased from Sigma–Aldrich Chemicals, USA with an average particle size of 20 μm. *N*,*N*-dimethylformamide (DMF) and sulfuric acid were used as received.

The Preparation of Nanocrystalline Cellulose (NCC)

Nanocrystalline cellulose (NCC) was obtained by acid hydrolysis of MCC according to the reported preparation process.[38] The typical procedure for preparing NCC is described as follows: 5 g of MCC was mixed with 100 mL 64% (w/v) sulfuric acid and stirred for 1 h at 45°C. After hydrolysis, the suspension was diluted with distilled water and successively centrifuged at 10,000 rpm for 10 min to remove the excess sulfuric acid until the supernatant became turbid. Dialysis against distilled water for several days until the pH value was constant, the sample was then freeze-dried.

Preparation of PPC/NCC Composites

Dried NCC was dispersed into DMF under ultrasound (about 10 min at 30% power input) with a sonifier. The resulting suspension is neither sediment nor flocculate, and then NCC of 1, 3, 5, 10, 20, and 30 wt % of PPC was added and stirring for 2 h at 70°C. Afterward, the solvent was distilled out in vacuum. The composites were obtained after dried at 80°C for 12 h, and denoted as PPC/1NCC, PPC/3NCC, PPC/5NCC, PPC/10NCC, PPC/20NCC, and PPC/30NCC respectively.

Thermal Degradation Test

As seen in Figure 2, about 20 mg samples were added to the NMR tubes. Nitrogen was filled to NMR tube for driving air completely. Afterward, NMR tube was sealed with a rubber hose which has a plug on the other end. And then set the bottom of the NMR tube into the oil bath with a temperature of 200°C for 4 h. Because PC, which was generated by PPC decomposition, has a boiling point of 242°C, could not be evaporated out in our system. After it cooled to the room temperature, 0.6 mL $CDCl_3$ was added for ^1H NMR test.

Characterizations

Transmission electron microscopy (TEM, Philips EM 400T) was performed to investigate the morphology of NCC. A drop of fully dispersed suspension (~0.01 g mL^{-1}) was air-dried on a copper grid (230 meshes) with carbon coated and then stained with a 1% phosphotungstic acid. Fourier transform infrared spectroscopy (FT-IR) spectra were recorded in a Bruker Vector 22 FTIR spectrometer. Typically, 32 scans were signal-averaged to reduce spectral noise. Samples were measured in the form of thin films. Differential scanning calorimetry (DSC) was taken on a DSCQ200 quipped with a liquid nitrogen cooling system. Nearly 3–5 mg of samples were placed in aluminum pans. Each sample was firstly heated to 100°C and kept for 5 min, then it

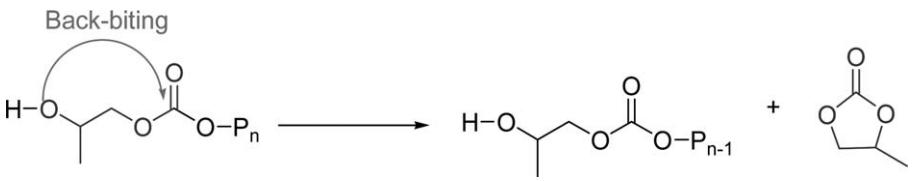

Scheme 2. PPC heat decomposition via the backbiting mechanism.

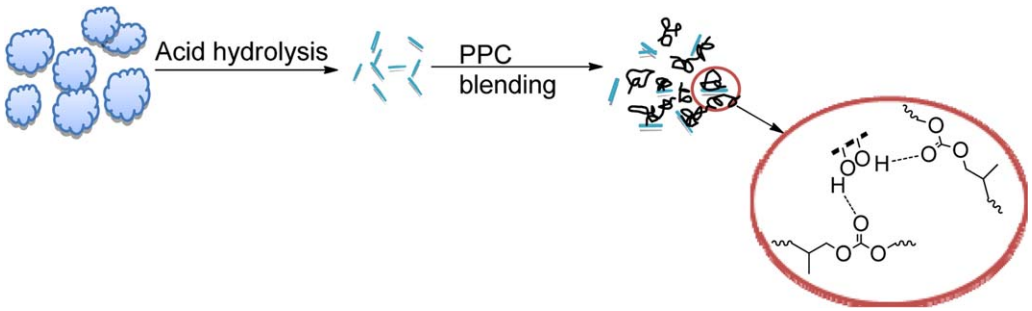

Figure 1. The cartoon of the acid hydrolysis of MCC and the blending of NCC with PPC. [Color figure can be viewed in the online issue, which is available at wileyonlinelibrary.com.]

was cooled down to 0°C and so forth twice, with the cooling and heating rates of both 10°C min^{-1}. Dynamic thermogravimetric (TGA) measurements were carried out under a nitrogen atmosphere (120 mL min^{-1}). Samples were heated from 25 to 600°C at a heating rate of 10°C min^{-1} under nitrogen atmosphere. ^1H NMR spectra of the products were obtained on a Bruker Advance DMX 400-MHz spectrometer using $CDCl_3$ as solvent and TMS as internal reference. X-ray powder diffraction (XRD) with Cu $K\alpha_1$ radiation ($\lambda = 1.54060$ Å) was used, where the angle 2θ was scanned between 5 and 70° and the scanning rate was 6° min^{-1}.

RESULTS AND DISCUSSION

For preparing the PPC/NCC composites, NCC was synthesized by acid hydrolysis of microcrystalline cellulose (MCC) based on the reported method.[38] The yield of NCC was 80% and it is light white powder. Figure 3 shows the TEM image of the obtained NCC. It is rod-like structure with a length of about 50–200 nm and width of about 10 nm.

X-ray diffraction (XRD) was applied to analysis the crystallinity of NCC, as shown in Figure 4. In both curves, three peaks were observed at $2\theta = 14.9, 16.2, 22.5°$, corresponding to three crystal face (101), (10$\bar{1}$), (002) that belongs to a Cellulose I structure. The crystallinity index and crystal dimension were calculated based on the reported method,[33] and the calculated results are summarized in Table I. The crystallinity index of NCC is 63 and bigger than that of MCC (55), indicating that the removal of the amorphous part in MCC. Correspondingly, the grain size of NCC was calculated as 5.6, which was smaller than that of MCC, also means the exfoliation of the amorphous region of MCC by acid hydrolysis. Both the TEM image and XRD pattern proved that NCC was successfully prepared.

Because NCC could be dispersed in DMF very well by sonication and PPC could be completely dissolved into DMF, both components were blended in DMF. The PPC/NCC blends with various NCC contents were obtained after complete removal of DMF.

To investigate the hydrogen bonding interaction between PPC and NCC in the resultant composite, FT-IR spectrum was performed for a thin film of PPC/30NCC blend. Figure 5 shows the FT-IR spectra of PPC, NCC, PPC/30NCC blend, and a control sample of PPC and MCC (30 wt %) (denoted as PPC/30MCC) prepared by using the same blending method. The characteristic peak at 1750 cm^{-1} could be ascribed to the stretching vibration of the carbonyl group of PPC. Such IR

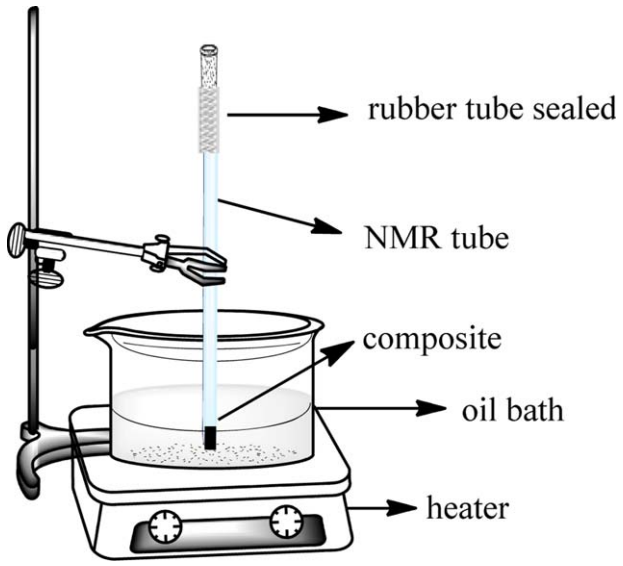

Figure 2. The setup for testing the thermal decomposition of PPC/NCC nanocomposites. [Color figure can be viewed in the online issue, which is available at wileyonlinelibrary.com.]

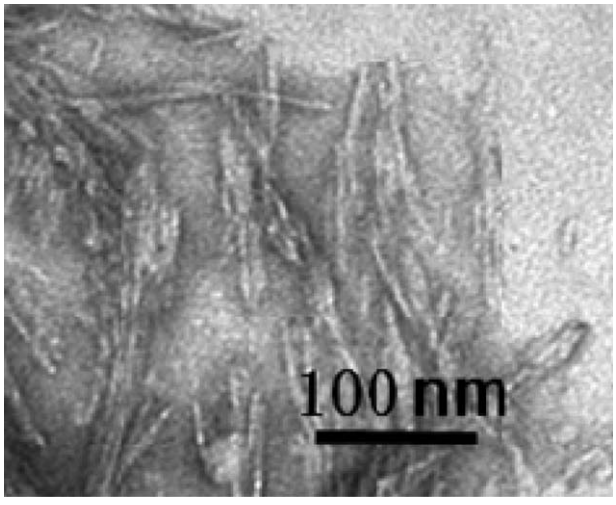

Figure 3. TEM image of NCC prepared by acid hydrolysis of MCC from cotton.

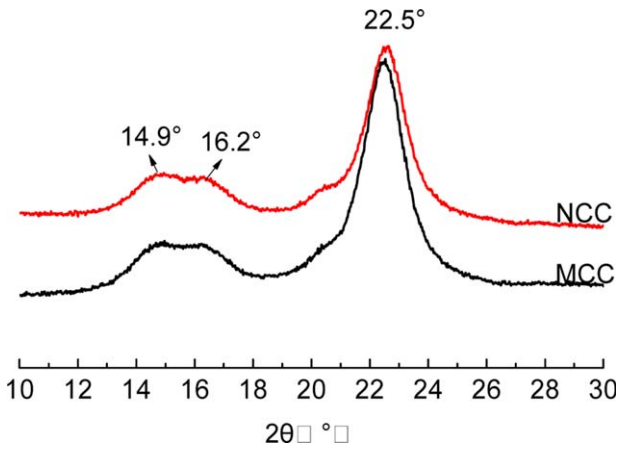

Figure 4. X-ray diffraction patterns f MCC and NCC. [Color figure can be viewed in the online issue, which is available at wileyonlinelibrary.com.]

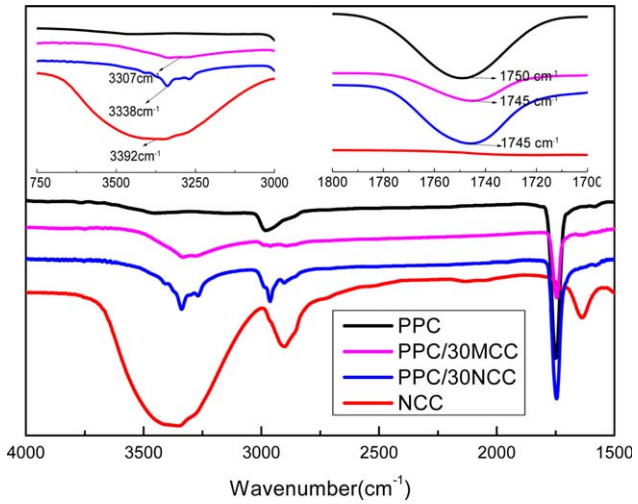

Figure 5. The FT-IR spectra of PPC, NCC and the composites of PPC/30NCC and PPC/30MCC. [Color figure can be viewed in the online issue, which is available at wileyonlinelibrary.com.]

peak shifted to 1745 cm^{-1} when it was blended with 30 wt % NCC. Moreover, the wide IR peak of NCC at about 3500 cm^{-1}, which is attributed to the —OH group of cellulose, split to several peaks after blending. This may imply several hydrogen bonding interactions such as —OH···OH—, —OH···O═C— in the PPC/30NCC blend formed. The control sample of PPC/30MCC showed the similar shift of the carbonyl stretching absorption with that of PPC/30NCC composite, however, no clear splits of IR peak at 3500 cm^{-1} were observed. This may indicate a relatively weak hydrogen bonding interaction. It is accepted that nano-sized NCC provided more surface area and probability to form hydrogen bonding than micro-sized MCC. Hence, we thought that the strong hydrogen bonding interaction of PPC and NCC could bind PPC chains onto the surface of NCC tightly in a nanometer scale, which would inhibit the thermal decomposition of PPC via "unzipping" manner. This was evident by the following evidences.

The glass transition temperatures (T_gs) of PPC and PPC/NCC composites were determined by differential scanning calorimetry (DSC) at a heating rate of 10°C under nitrogen atmosphere, as shown in Table II. T_gs of all PPC/NCC composites were in the range of 32.4–33.9°C that were very close to that of pure PPC (33.3°C). That is, the variations of T_g values of PPC in these composites were rather small. It is believed that rod-like rigid crystalline of NCC and hydrogen bonding interaction between PPC and NCC had a neglected effect on the chain segment motion of PPC.[48] Surprisingly, T_g value of PPC/30MCC blend was only 14°C and dramatically lower than that of pure PPC, which is not good in its application. Presumably, noncrystalline part of MCC might act as a plasticizer for PPC and thus caused a sharp T_g decrease of PPC.

Figure 6 shows the thermal gravimetric (TGA) curves of PPC, NCC and PPC/NCC composites with different weight percentage of NCC. The 5% weight loss temperatures ($T_{5\ wt\%}$s) and the maximum weight loss temperatures (T_{max}s) of these samples are collected in Table II. $T_{5\ wt\%}$ and T_{max} of pure PPC are 225.6 and 241.0°C, respectively, while $T_{5\ wt\%}$ and T_{max} of NCC are 242.1 and 305.2°C, respectively. That is, NCC is more heat resistant than PPC, which is favorable to the enhancement of the thermal properties of the composites. It was pleased to see that $T_{5\ wt\%}$ and T_{max} of PPC were clearly improved even if 1 wt % NCC was incorporated, as shown in Figure 4, $T_{5\ wt\%}$ and T_{max} of PPC/1NCC are 247.6 and 275.8°C, respectively. With

Table I. Crystallinity and Crystal Dimension of MCC and NCC

Sample	X_c[a] (%)	D[b](nm)(002)
MCC	55	6.1
NCC	63	5.6

[a] X_c: crystallinity, $X_c = (I_{002} - I_{am})/I_{002}$, I_{002} is the overall area of the peak at 2θ about 22.5°, I_{am} is the area of the amorphous region.[33]
[b] D: crystal dimension, calculated according to Scherrer formula. $D_{hkl} = \lambda k/\beta\cos\theta$, $\lambda = 0.154$ nm. $K = 0.9$, β = half peak width at 2θ about 22.5°.

Table II. Thermal Properties of NCC Reinforced PPC Composites at Different Filler Loading

Samples	T_g (°C)	$T_{5\ wt\ \%}$ (°C)	T_{max} (°C)	W_{cPc}[a] (%)
PPC	33.3	225.6	241.0	48
PPC/1NCC	33.9	247.6	275.8	28
PPC/3NCC	32.6	259.5	284.1	19
PPC/5NCC	32.4	258.6	286.4	13
PPC/10NCC	33.4	261.3	289.4	11
PPC/20NCC	32.8	265.1	299.2	9
PPC/30NCC	33.4	265.2	301.8	7
NCC	-	242.1	305.2	-
PPC/30MCC	14.0	256.0	299.0	15

The T_{max} was calculated by derivation of weight remaining to temperature.
[a] The weight percentage of cyclic propylene carbonate in total product (W_{cPC}, wt %) were calculated by integrating the ^{1}H NMR peak area: $W_{cpc} = 102A_{1.5}/[102(A_{5.0} + A_{4.2} - 2A_{4.6} + A_{1.5}) + 58A_{3.5}]$.[1]

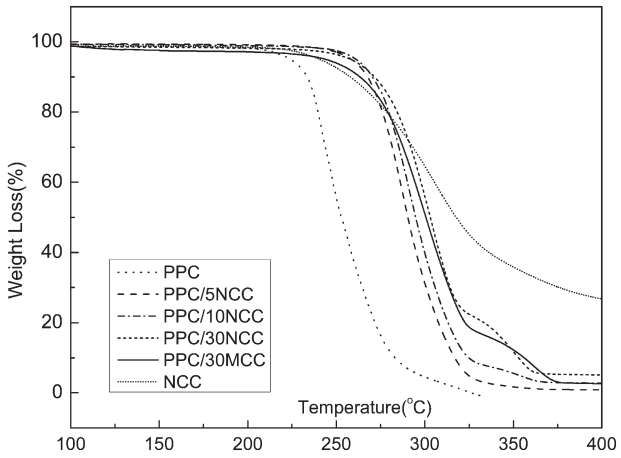

Figure 6. Thermal gravimetric curves of pure PPC and NCC reinforced PPC composites at different filler loading.

increasing the NCC content in the composite, both $T_{5\ wt\%}$ and T_{max} of the composites increased from 247.6 to 265.2°C and from 275.8 to 305.2°C, respectively. Moreover, the thermal decomposition parameters of all PPC/NCC composites with 1–30 wt % NCC were higher than those of pure PPC and NCC. This could be ascribed to the hydrogen bonding interaction of PPC and NCC. Moreover, the control example of PPC/30MCC blend presented improved $T_{5,\ wt\%}$ of 256.0°C, which was lower than those of PPC/NCC composites with 3–30 wt % NCC, which could be attributed to the insufficient hydrogen-bonding interaction of PPC and MCC. In this protocol, the chain scission of PPC via backbiting route was dramatically inhibited. Because the end hydroxyl group of PPC had not been capped, the hydrogen-bonding interaction of PPC and NCC was the key factor to the inhibition of thermal decomposition of PPC in the composites.

For quantitatively evaluating the decomposition extent of the above PPC/NCC composites in the case of isothermal process, an isothermal decomposition experiment was designed, as described in the experimental part. Herein, the temperature was set as 200°C which was higher than 170°C which is considered to be the ceiling point of PPC decomposition during heat process (the mechanical decomposition of PPC was not considered in this text). After isothermal decomposition, ^{1}H NMR characterization of these samples was carried out directly, and the results are shown in Figure 7.

Figure 7 shows the ^{1}H NMR spectra of the pure PPC, PPC/NCC blends with 1–30 wt % NCC and PPC/30MCC blend after heated at 200°C for 4 h. The attribution of each peaks at ^{1}H NMR spectrum of the pure PPC (curve A) after heated were as follows: 1.3 ppm [3H, CH_3(d)], 4.2 ppm [2H, $CH_2(CO_3)$(e)], 5.0 ppm [1H, $CH(CO_3)$(f)], 3.5 ppm [3H, CH_2CH(b, c)], and 1.2ppm [3H, CH_3(a)]. We observed that the characteristic NMR peaks of PC were located at: 1.5 ppm [3H, CH_3(g)], 4.0 ppm [1H, $CH_2(CO_3)$(h)], 4.6 ppm [1H, $CH_2(CO_3)$(i)], and 4.9 ppm [1H, CH (CO_3)(j)]. On the basis of the calculation method for PC content in the product we reported,[9] 48% PC was produced for pure PPC after heating, which means that pure PPC was easy to be decomposed to PC at such severe isothermal heating

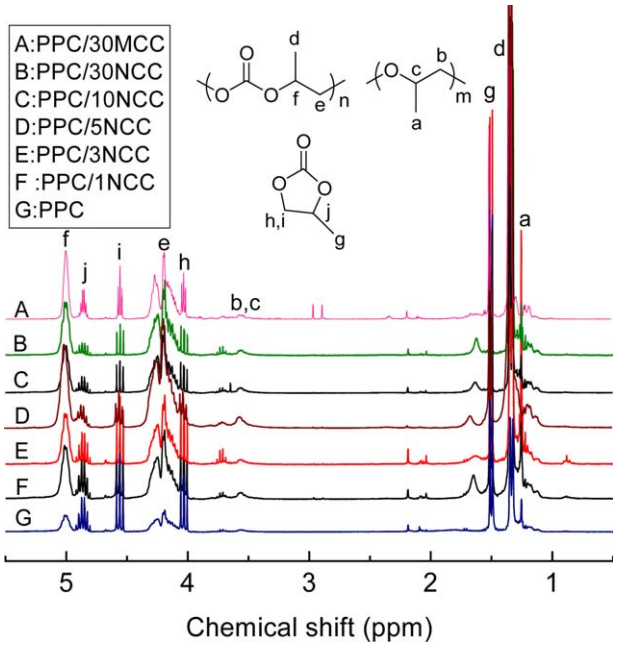

Figure 7. The ^{1}H NMR spectra of pure PPC and NCC (or MCC) reinforced PPC composites at different filler loading. [Color figure can be viewed in the online issue, which is available at wileyonlinelibrary.com.]

condition because random chain scission would be dominant at such high temperature. Surprisingly, even 1 wt % NCC was incorporated, the production of PC after heating decreased to 28 wt % (curve F). The more the NCC incorporated, the less the PC produced, as seen in Table II. For PPC/30NCC composite, only 7 wt % PC was produced. However, for PPC/30MCC composite, there are still 15 wt % PC produced. The isothermal experimental results also disclosed that the effect of the hydrogen bonding interaction on the inhibition of thermal

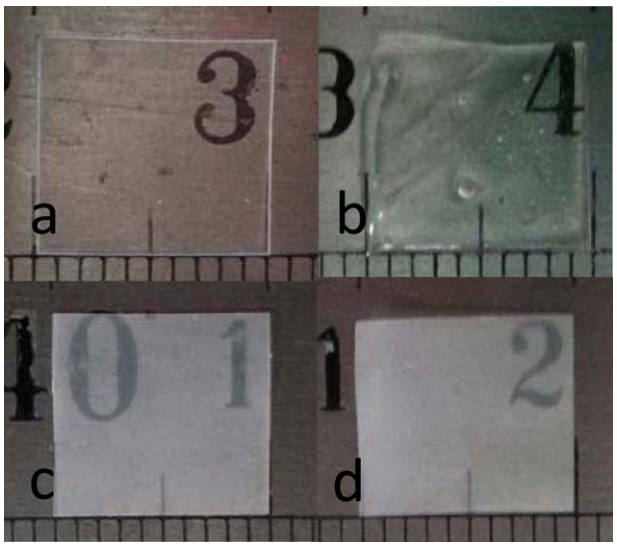

Figure 8. Optical photographs of pure PPC (a, b) and PPC/30NCC(c, d) a: PPC(before heating) b: PPC(after heating); c: PPC/30NCC(before heating) d: PPC/30NCC(after heating). [Color figure can be viewed in the online issue, which is available at wileyonlinelibrary.com.]

decomposition of PPC in such nanocomposites. Although a single hydrogen bond is weak, considerable amounts of hydrogen bond in the blend presented a strong inhibitory effect on the PPC decomposition via random chain scission route at high temperatures (including backbiting mechanism). Therefore, blending of PPC with NCC is an effective method for inhibiting the decomposition of PPC during its heat process, which is different from the method via capping the hydroxyl group of PPC.[21,49]

Another problem relating to the application of PPC is that it is easy to be deformed after heating due to its low T_g (30–45°C). We observed that the incorporation of NCC could effectively inhibit the shape deformation after heating. Figure 8 shows optical photographs of pure PPC and PPC/30NCC composite with an area of about $1 \times 1 \times 0.1$ cm^3 (a and c). After heated at 110°C in oven for 4 h, PPC deformed severely as shown as Figure 8(b), while the shape of the PPC/30NCC composite kept unchanged (d in Figure 8).

CONCLUSIONS

In this study, a biodegradable PPC/NCC nanocomposite was prepared and characterized. The hydrogen bonding interaction between NCC and PPC was confirmed and proved to be effective to the improvement of thermal properties of the resultant PPC/NCC nanocomposite. The chemistry involved in this blend is multiple hydrogen bonding interaction of PPC with NCC, rather than the "capping" of the hydroxyl group of PPC.

REFERENCES

1. Luinstra, G. A. *Polym. Rev.*, **2008**, *48*, 192.
2. Qin, Y. S.; Wang, X. H. *Biotechnol J* **2010**, *5*, 1164.
3. Sakakura, T.; Choi, J. C.; Yasuda, H. *Chem. Rev.*, **2007**, *107*, 2365.
4. Liu, B. Y.; Gao, Y. H.; Zhao, X.; Yan, W. D.; Wang, X. H. *J. Polym. Sci. Polym. Chem.*, **2010**, *48*, 359.
5. Wang, S.; Du, L.; Zhao, X.; Meng, Y.; Tjong, S. *J. Appl. Polym. Sci.*, **2002**, *85*, 2327.
6. Zhu, Q.; Meng, Y. Z.; Tjong, S. C.; Zhao, X. S.; Chen, Y. L. *Polym. Int.*, **2002**, *51*, 1079.
7. Meng, Y.; Du, L.; Tiong, S.; Zhu, Q.; Hay, A. S. *J. Polym. Sci. A Polym. Chem.*, **2002**, *40*, 3579.
8. Chen, S. M.; Tan, L.; Qiu, F. R.; Jiang, X. L.; Wang, M.; Zhang, H. D. *Polymer*, **2004**, *45*, 3045.
9. Zhang, X. H.; Wei, R. J.; Sun, X. K.; Zhang, J. F.; Du, B. Y.; Fan, Z. Q.; Qi, G. R. *Polymer*, **2011**, *52*, 5494.
10. Gu, L.; Qin, Y.; Gao, Y.; Wang, X.; Wang, F. *Chin. J. Chem.*, **2012**, *30*, 2121.
11. Liu, S.; Wang, J.; Huang, K.; Liu, Y.; Wu, W. *Polym. Bull.*, **2011**, *66*, 327.
12. Ma, X.; Yu, J.; Wang, N. *J. Polym. Sci. B Polym. Phys.*, **2005**, *44*, 94.
13. Chen, S.; Xiao, M.; Wang, S.; Han, D.; Meng, Y. *J. Polym. Res.*, **2012**, *19*, 1.
14. Darensbourg, D. J.; Poland, R. R.; Strickland, A. L. *J. Polym. Sci. A Polym. Chem.*, **2011**, *50*, 127.
15. Shi, L.; Lu, X. B.; Zhang, R.; Peng, X. J.; Zhang, C. Q.; Li, J. F.; Peng, X. M. *Macromolecules*, **2006**, *39*, 5679.
16. Hwang, Y.; Jung, J.; Ree, M.; Kim, H. *Macromolecules*, **2003**, *36*, 8210.
17. Hwang, Y.; Ree, M.; Kim, H. *Catal Today*, **2006**, *115*, 288.
18. Liu, S.; Xiao, H.; Huang, K.; Lu, L.; Huang, Q. *Polym. Bull.*, **2006**, *56*, 53.
19. Lu, L.; Huang, K. *Polym. Int.*, **2005**, *54*, 870.
20. Sun, X. K.; Zhang, X. H.; Chen, S.; Du, B. Y.; Wang, Q.; Fan, Z. Q.; Qi, G. R. *Polymer*, **2010**, *51*, 5719.
21. Gao, F.; Zhou, Q.; Qin, Y.; Wang, X.; Zhao, X.; Wang, F. *Acta Polym. Sin.*, **2011**, *7*, 772.
22. Darensbourg, D. J.; Wei, S. H. *Macromolecules*, **2012**, *45*, 5916.
23. Wang, X.; Du, F.; Jiao, J.; Meng, Y.; Li, R. *J. Biomed. Mater. Res. B Appl. Biomater.*, **2007**, *83*, 373.
24. Ma, X.; Yu, J.; Wang, N. *J. Polym. Sci. B Polym. Phys.*, **2006**, *44*, 94.
25. Zhang, Z.; Mo, Z.; Zhang, H.; Wang, X.; Zhao, X. *Macromol. Chem. Phys.*, **2003**, *204*, 1557.
26. Ge, X.; Li, X.; Zhu, Q.; Li, L.; Meng, Y. *Polym. Eng. Sci.*, **2004**, *44*, 2134.
27. Ma, X.; Chang, P. R.; Yu, J.; Wang, N. *Carbohydr. Polym.*, **2008**, *71*, 229.
28. Peng, S.; Wang, X.; Dong, L. *Polym. Compos.*, **2005**, *26*, 37.
29. Ge, X.; Zhu, Q.; Meng, Y. *J. Appl. Polym. Sci.*, **2006**, *99*, 782.
30. Nishino, T.; Matsuda, I.; Hirao, K. *Macromolecules*, **2004**, *37*, 7683.
31. Eichhorn, S.; Baillie, C.; Zafeiropoulos, N.; Mwaikambo, L.; Ansell, M.; Dufresne, A.; Entwistle, K.; Herrera-Franco, P.; Escamilla, G.; Groom, L. *J. Mater. Sci.*, **2001**, *36*, 2107.
32. Klemm, D.; Kramer, F.; Moritz, S.; Lindström, T.; Ankerfors, M.; Gray, D.; Dorris, A. *Angew. Chem. Int. Ed.*, **2011**, *50*, 5438.
33. Lee, S. Y.; Mohan, D. J.; Kang, I. A.; Doh, G. H.; Lee, S.; Han, S. O. *Fibers Polym.*, **2009**, *10*, 77.
34. Favier, V.; Chanzy, H.; Cavaille, J. Y. *Macromolecules* **1995**, *28*, 6365.
35. Petersson, L.; Kvien, I.; Oksman, K. *Compos. Sci. Technol.*, **2007**, *67*, 2535.
36. Terech, P.; Chazeau, L.; Cavaille, J. *Macromolecules*, **1999**, *32*, 1872.
37. Tokoh, C.; Takabe, K.; Fujita, M.; Saiki, H. *Cellulose*, **1998**, *5*, 249.
38. Dong, X. M.; Revol, J.-F.; Gray, D. G. *Cellulose*, **1998**, *5*, 19.
39. Dong, X. M.; Kimura, T.; Revol, J. F.; Gray, D. G. *Langmuir*, **1996**, *12*, 2076.
40. Azizi Samir, M. A. S.; Alloin, F.; Sanchez, J.-Y.; El Kissi, N.; Dufresne, A. *Macromolecules*, **2004**, *37*, 1386.
41. Bondeson, D.; Mathew, A.; Oksman, K. *Cellulose*, **2006**, *13*, 171.

42. Lima, M. M. D.; Borsali, R. *Macromol. Rapid Commun.*, **2004**, *25*, 771.

43. Nishino, T.; Takano, K.; Nakamae, K. *J. Polym. Sci. Polym. Phys.*, **1995**, *33*, 1647.

44. Huang, Z. M.; Zhang, Y. Z.; Kotaki, M.; Ramakrishna, S. *Compos. Sci. Technol.*, **2003**, *63*, 2223.

45. Chazeau, L.; Paillet, M.; Cavaille, J. *J. Polym. Sci. B Polym. Phys.*, **1999**, *37*, 2151.

46. Li, W.; Yue, J.; Liu, S. *Ultrason. Sonochem.*, **2011**, *19*, 479.

47. Azizi Samir, M. A. S.; Alloin, F.; Sanchez, J. Y.; Dufresne, A. *Polymer*, **2004**, *45*, 4149.

48. Chen, L. J.; Qin, Y. S.; Wang, X. H.; Zhao, X. J.; Wang, F. S. *Polymer*, **2011**, *52*, 4873.

49. Yao, M.; Mai, F.; Deng, H.; Ning, N.; Wang, K.; Fu, Q. *J. Appl. Polym. Sci.*, **2011**, *120*, 3565.